

## **Appendix A: Supplementary Data**

### **Hydrophobic Fouling Resistant Electrospun Nanofiber Membranes from Poly(vinylidene fluoride)/Polyampholyte Blends**

Anuja S Jayasekara<sup>1</sup>, Luca Mazzaferro<sup>2</sup>, Ryan O'Hara<sup>2</sup>, Ayse Asatekin<sup>2</sup>, Peggy Cebe<sup>1</sup>

<sup>1</sup> Department of Physics & Astronomy

<sup>2</sup> Department of Chemical & Biological Engineering

Tufts University, Medford MA 02155

Contact Information: [peggy.cebe@tufts.edu](mailto:peggy.cebe@tufts.edu)

## **S1. SEM Fiber Diameter Analysis**

The fiber images in our study show that beads are often observed. Depending upon the number and size of beads, it is possible that beads contain a lot of polymer mass, leading to thinner fibers in between the beads. For proper fiber diameter analysis, the SEM images should be examined in two ways: case 1, to determine the bulk average size of both fibers and beads taken together (**Fig. S1, S2**); and case 2, to determine the size of fibrils alone under conditions where the beads are excluded (**Fig. S3**). We will refer to case 1 as “bulk fiber diameter” analysis and case 2 as “fibril diameter” analysis. **Figure S1** illustrates the method used for Case 2, bulk fiber analysis, and **Figure S2** shows the histograms of the bulk fiber diameter distribution in each electrospun fiber mat.

### **Case 1: Bulk fiber diameter measurements**

In DiameterJ analysis, an SEM image (**Fig. S1-A**) is first segmented into 24 images with pure black and white pixels (three categories with eight images in each category) as shown in **Fig. S1-B**. A set of three images from each category was selected by the authors, using their best judgment, to represent the true fiber structure in the sample. These nine images are shown in **Fig. S1-B** with a red outline. Using these nine segmented images, the average diameter of the bulk (including beads) was determined for each sample using the DiameterJ plug in of ImageJ. Histograms of the bulk fiber diameters, including the beads, are shown for each electrospun fiber mat in **Fig. 2A-G**.

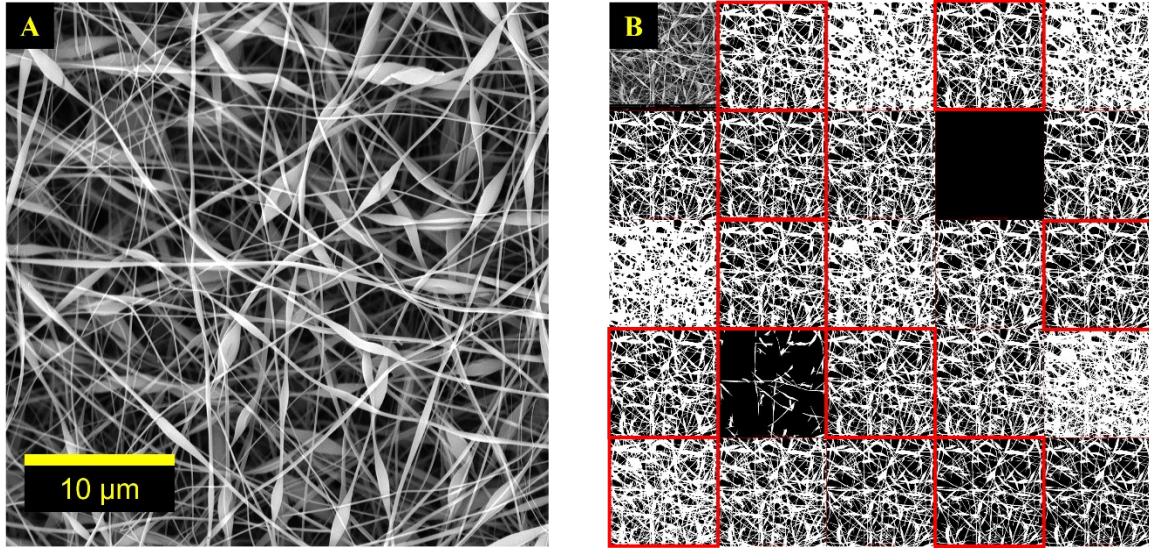


**Figure S1:** A) SEM image of PVDF00 at  $\times 7500$  magnification; B) Montage of the segmented black and white pixelated images of the same SEM image but with the scale bar removed. The nine segmented images that were considered in the DiameterJ analysis are outlined in red boxes.

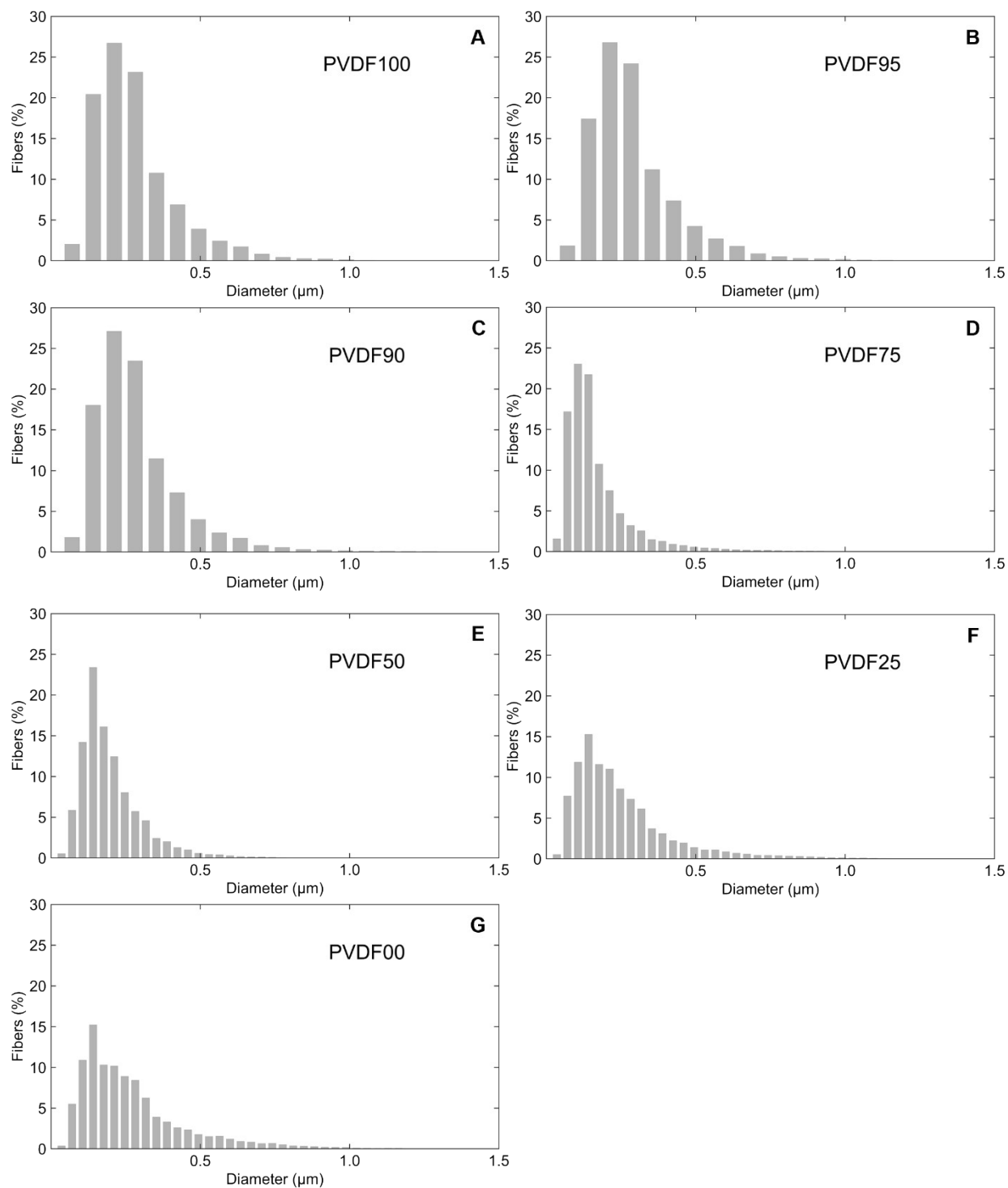


**Figure S2:** Histograms of bulk fiber diameter distribution, including beads, for: A) PVDF100; B) PVDF95; C) PVDF90; D) PVDF75; E) PVDF50; F) PVDF25; G) PVDF00.

## Case 2: Fibril diameter measurements.

Next, an in-depth analysis was done to determine the case 2 “fibril diameter” distribution. Since the bulk fiber diameter values include the bead diameters, a method to eliminate the beads was carried out to determine the fibril diameter values. As shown in **Fig. S3 (A-B)**, a cut-off diameter value was measured and defined for a fiber as it widens to form a bead. A line was drawn along the fiber passing into the bead (**Fig S3-B**, red dashed line PQ) and then another line was drawn perpendicular to PQ at the critical point where the fiber starts to flare out and turn into a bead (**Fig S3-B**, double arrow line RS). The length of RS is defined as the cut-off diameter value, the largest diameter that can still be considered to be a fiber and not a bead. Using the Specific Radius Identifier in DiameterJ, the fibers with diameters below the cut-off diameter value (defined as “fibrils”) are highlighted in red in the segmented images. As shown in **Fig S3-C**, this analysis has successfully excluded the beads, and avoids considering them in the analysis of the fibril diameter.

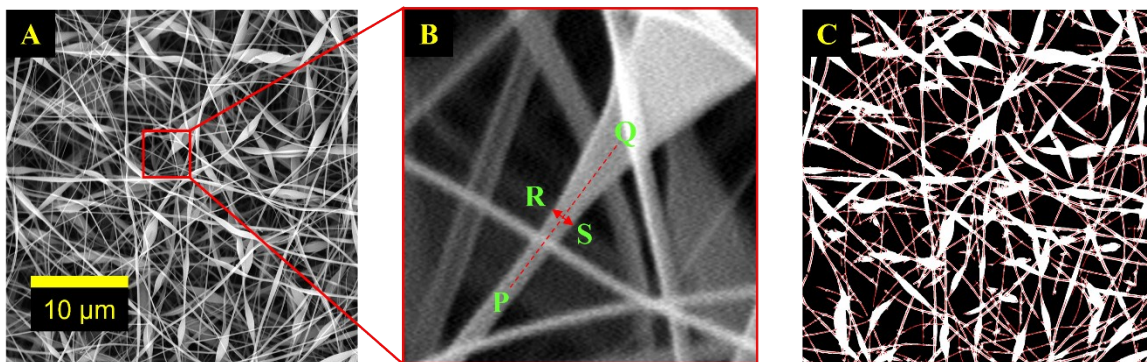


**Figure S3:** A) SEM image of PVDF00 at  $\times 7500$  magnification; B) Zoomed in image of a fiber turning into a bead. Red dashed line PQ is drawn along the fiber into the bead and double arrow RS is the cut-off diameter drawn normal to PQ; C) Segmented image of the same SEM image with scale bar removed, and with fibrils highlighted in red.

Then the average fibril diameter (without beads) was determined by taking the mean value of the diameters below the cut-off diameter value. The standard deviations of the bulk and fibril diameter distributions are presented as the uncertainty of the average bulk fiber diameter and the average fibril diameter measurements. These data are presented in **Table 1** in the main manuscript.

## S2. SEM Porosity Analysis

The same set of nine segmented images used for diameter analysis in each sample was also used for the porosity analysis. An example SEM image is shown in **Fig. S4A** for PVDF00. One of the nine segmented images is shown in **Fig. S4-B**. **Fig S4-C** shows the DiameterJ output image of the SEM image with every pore marked in red. Large black void areas in **Fig. S4B** are counted as “pores” if they are interior to the image; they are not counted as “pores” if they appear at the edge of the image.

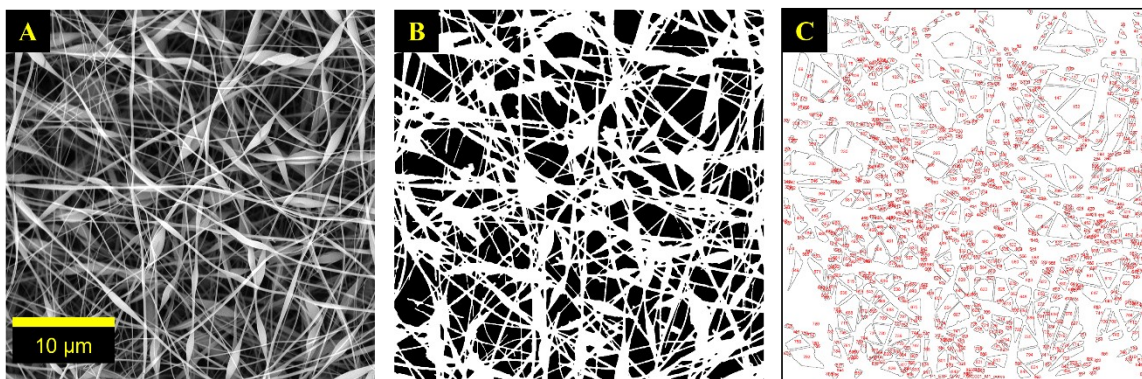


**Figure S4:** A) SEM image of PVDF00 at  $\times 7500$  magnification; B) Segmented image of the same SEM image with scale bar removed; C) Pores present in the segmented image. Each pore is numbered in red.

Pore data from all segmented images were used in estimating the average pore area. To estimate the uncertainty in mean pore area, a bootstrapping technique was used because the data are highly skewed. Pore data histograms are shown in **Fig. S5**. Pore data are shown in **Table S1**.

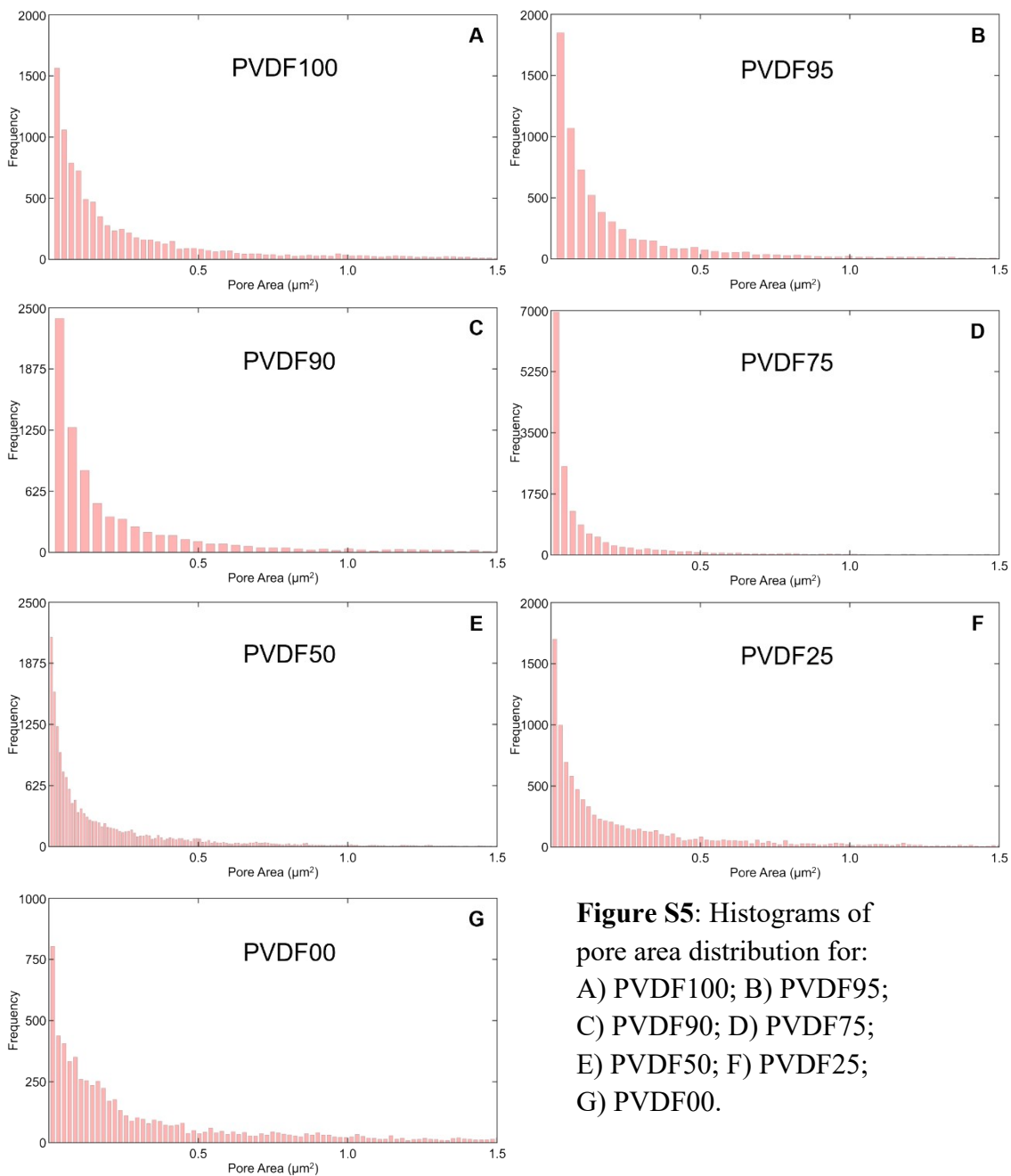


**Figure S5:** Histograms of pore area distribution for: A) PVDF100; B) PVDF95; C) PVDF90; D) PVDF75; E) PVDF50; F) PVDF25; G) PVDF00.



**Table S1:** Pore data values of PVDF/r-PAC blends

Sample	Average No. of Pores per Image <sup>a</sup>	Pore Density <sup>b</sup> ( $\times 10^5 \text{ mm}^{-2}$ )	Average Pore Area ( $\mu\text{m}^2$ )	Pores with Areas below the Avg. Pore Area (%)
PVDF00	828	6.35	$0.67 \pm 0.03$	74
PVDF25	1125	8.62	$0.48 \pm 0.02$	77
PVDF50	1996	15.3	$0.27 \pm 0.01$	73
PVDF75	1828	14.0	$0.26 \pm 0.02$	83
PVDF90	907	6.95	$0.49 \pm 0.04$	82
PVDF95	791	6.06	$0.46 \pm 0.03$	82
PVDF100	1061	8.13	$0.43 \pm 0.02$	77

<sup>a</sup> The nine images shown in Fig. S1 were examined for pores and the average number of pores per image is listed in the table. The magnification of the images was the same for all samples.

<sup>b</sup> SEM images were converted from pixel units to  $\text{mm}^2$ .

All SEM images can be found via the following link

<https://doi.org/10.17605/OSF.IO/E683P>

### S3. Viscosity Analysis

The viscosity of each electrospinning solution was measured using a rotational viscometer (IKA lo-vi, Wilmington, NC). A volume of 2.1 mL from each solution (10 wt.% of solid polymer in dimethylformamide/methanol 13/01 v/v) was poured into the viscosity chamber



and the spindle was rotated at a rate of 200 rpm for 10 minutes and the dynamic viscosity was measured every 30 s. The chamber was maintained at a constant temperature of 18 °C. The mean dynamic viscosity was calculated averaging all viscosity values collected over 10 mins and shown in **Table S2**. The standard deviation of the viscosities is presented as the uncertainty.

**Table S2:** Mean dynamic viscosity of sample solutions

Sample	Mean Dynamic Viscosity (mPa.s)
PVDF00	240.8 ± 2.1
PVDF25	359.4 ± 2.0
PVDF50	477.6 ± 2.5
PVDF75	554.9 ± 3.3
PVDF90	568.9 ± 5.3
PVDF95	399.1 ± 2.2
PVDF100	394.0 ± 3.7

The relationship between the average fibril diameter (black squares) and the solution viscosity (red circles) is shown in **Fig. S6** as a function of r-PAC content. The viscosity increases with the addition of r-PAC up to PVDF90 which shows the highest mean dynamic viscosity of 568.9 mPa.s ± 5.3 mPa.s. PVDF75 also shows a similar viscosity as PVDF90. The average fibril diameter decreases from PVDF100 to PVDF75. The viscosity decreases as more r-PAC is introduced to the solution and at the same time, the average fibril diameter increases.

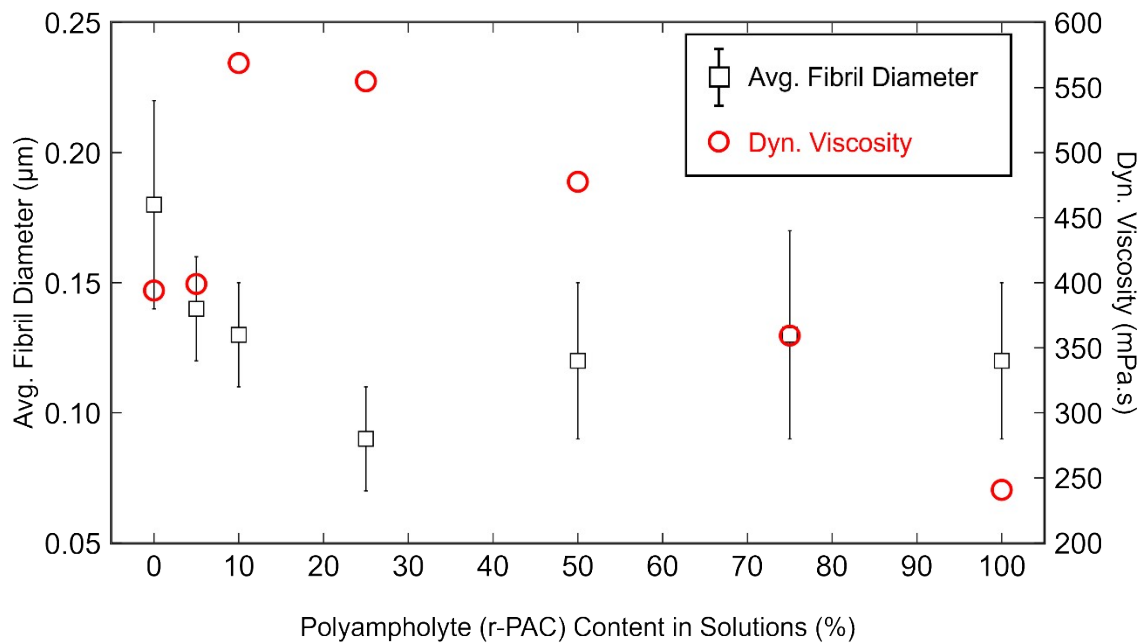


**Figure S6:** The variation of the mean fibril diameter of electrospun mats (black squares, left axis) and the dynamic viscosity of the solutions (red circles, right axis) with the polyampholyte (r-PAC) percentage in each sample. The percentage refers to the comparison of the r-PAC content to the PVDF content in the blends.

**S4. Please follow the link to access the videos of the contact angle measurements of each sample with oil (dodecane)**

<https://doi.org/10.17605/OSF.IO/E683P>